Science of the Total Environment 914 (2024) 169652

Contents lists available at ScienceDirect

Science of the Total Environment

journal homepage: www.elsevier.com/locate/scitotenv

Trophic transfer of rare earth elements in the food web of the Loire estuary (France)

Julie Rétif [a,*], Aurore Zalouk-Vergnoux [a], Abderrahmane Kamari [a], Nicolas Briant [b], Laurence Poirier [a]

[a] Nantes Université, Institut des Substances et Organismes de la Mer, ISOMer, UR 2160, F-44000 Nantes, France
[b] Ifremer, CCEM Contamination Chimique des Écosystèmes Marins, F-44000 Nantes, France

HIGHLIGHTS

- REE concentrations were the highest in primary producers and the lowest in fish.
- Trophic dilution of REEs was demonstrated with a corresponding TMS of −2.0.
- REE contribution was similar in all studied species: LREEs > HREEs > MREEs.
- Eu, Gd, Tb and Lu positive anomalies were reported in vertebrates and crustaceans.
- REE bioaccumulation in vertebrates' tissues was higher in gonads than in the muscle.

GRAPHICAL ABSTRACT

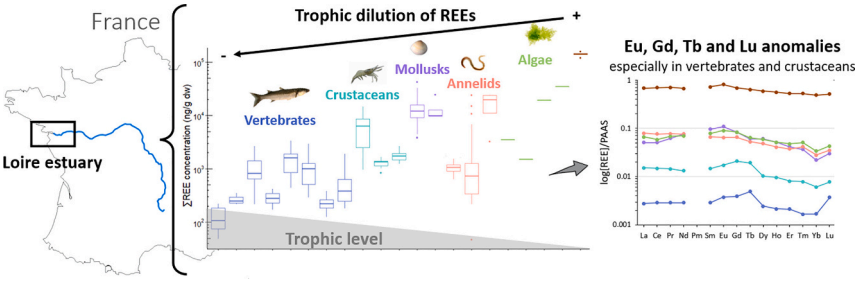

ARTICLE INFO

Editor: Damià Barceló

Keywords:
REEs
Bioaccumulation
Trophic dilution
Gd anomalies
Estuarine ecosystem

ABSTRACT

The increasing use of rare earth elements (REEs) in many industrial sectors and in medecine, causes discharges into the environment and particularly in estuarine areas subjected to strong anthropogenic pressures. Here, we assessed the distribution of REEs along the food web of the Loire estuary. Several species representative of different trophic levels were sampled: 8 vertebrates, 3 crustaceans, 2 mollusks, 3 annelids and 4 algae, as well as *Haploops sp.* tubes rather related to sediment. The total REE concentrations measured by ICP-MS were the highest in *Haploops sp.* tubes (141.1 ± 4.7 μg/g dw), algae (1.5 to 34.5 μg/g dw), mollusks (9.9 to 12.0 μg/g dw), annelids (0.7 to 19.9 μg/g dw) and crustaceans (1.4 to 6.3 μg/g dw) and the lowest in vetebrates (0.1 to 1.6 μg/g dw). The individual contribution of REEs was, however, similar between most studied species with a higher contribution of light REEs (76.7 ± 7.6 %) compared to heavy REEs (14.1 ± 3.7 %) or medium REEs (9.2 ± 5.8 %). Trophic relations were estimated by stable isotope analysis of C and N and the linear regression of $\delta^{15}N$ with total REE concentrations highlighted a trophic dilution with a corresponding TMS of −2.0. The tissue-specific bioaccumulation investigated for vertebrates demonstrated a slightly higher REE accumulation in gonads than in the muscle. Finally, positive Eu, Gd, Tb and Lu anomalies were highlighted in the normalized REE patterns of most studied species (especially in fish and crustaceans), which is consistent with results in the dissolved phase for Eu and Gd. These anomalies could either be due to anthropogenic inputs or to various bioaccumulation/elimination processes according to the specific species physiology. This study, including most of the trophic

* Corresponding author.
E-mail addresses: julie.retif@univ-nantes.fr (J. Rétif), aurore.zalouk-vergnoux@univ-nantes.fr (A. Zalouk-Vergnoux), abderrahmane.kamari@univ-nantes.fr (A. Kamari), Nicolas.Briant@ifremer.fr (N. Briant), laurence.poirier@univ-nantes.fr (L. Poirier).

https://doi.org/10.1016/j.scitotenv.2023.169652
Received 10 October 2023; Received in revised form 8 December 2023; Accepted 22 December 2023
Available online 28 December 2023

levels of the Loire estuary food web provides new insights on the bioaccumulation and trophic transfer of REEs in natural ecosystems.

1. Introduction

Rare earth elements (REEs) define a category of metals grouping together the fifteen lanthanides (from lanthanum (La) to lutetium (Lu)), to which scandium (Sc) and yttrium (Y) are commonly added because of similar geochemical behavior. REEs can be arranged depending on their molecular weight in three categories (Bru et al., 2015): the light REEs (LREEs: La, cerium (Ce), praseodymium (Pr), neodymium (Nd) and promethium (Pm)), the medium REEs (MREEs: samarium (Sm), europium (Eu) and gadolinium (Gd)) and the heavy REEs (HREEs: terbium (Tb), dysprosium (Dy), holmium (Ho), erbium (Er), thulium (Tm), ytterbium (Yb) and Lu). Despite its low molecular weight, Y is included in the HREEs because of its closer chemical and behavioral properties to HREEs than LREEs (Bru et al., 2015; Mehmood, 2018). All REEs have very similar chemical properties due to their comparable electronic configuration (partially filled 4f electron shell) providing remarkable electromagnetic and catalytic properties. These similarities are even stronger between elements belonging to the same category.

The rising interest of society to these elements, with an estimated increase of the demand and production of 6 % per year (Bru et al., 2015), gives REEs an essential role in the global economy. They are mostly used in the industry sector in permanent magnets, metallurgical alloys, catalytic converters, lasers, phosphors, batteries or glass polishing (Castor and Hedrick, 2006; Bru et al., 2015), but are also increasingly used in medicine, as contrast agent for MRI (magnetic resonance imaging) or in tomography, as well as in radionuclide therapy (Müller et al., 2018; Blomqvist et al., 2022). Although REEs are naturally present in the earth's crust, the increase of global extraction combined to anthropogenic uses (industrial, agricultural or medical) induce more releases into the environment, causing progressive enrichments in the aquatic ecosystems (Hatje et al., 2016; Lerat-Hardy et al., 2019) including both freshwater (*e.g.* La, Sm and Gd, Elbaz-Poulichet et al., 2002; Kulaksiz and Bau, 2013; Merschel and Bau, 2015; Lerat-Hardy et al., 2019) and seawater (*e.g.* Gd and Tb, de Baar et al., 1985; Alibo and Nozaki, 1999; da Costa et al., 2021). Wastewater treatment plants (WWTP), receiving hospital, domestic and industrial water effluents are now recognized as the main source of REEs in polluted aquatic systems (Kawasaki et al., 1998; Kümmerer and Helmers, 2000; Rabiet et al., 2009; Verplanck et al., 2010).

Studies on the abiotic compartments show globally higher REE levels in sediment compared to the water column (Censi et al., 2007; Amyot et al., 2017). The investigation of REEs in estuarine sediments from Spain, Mexico, Portugal, China and Brazil demonstrated a range of concentrations from 18 to 220 μg/g dry weight (Borrego et al., 2004; Marmolejo-Rodríguez et al., 2007; Brito et al., 2018; Chi et al., 2021; de Freitas et al., 2021; Santos et al., 2023). On the other hand, the order of magnitude of the concentrations measured in the dissolved phase of European estuaries and rivers was ng/L (Kulaksiz and Bau, 2013; Lerat-Hardy et al., 2019; Cánovas et al., 2020). However, despite the lower REE concentrations found in the water column, the anomalies are mostly quantified in the dissolved phase compared to the particulate phase or sediment (Elbaz-Poulichet et al., 2002; Censi et al., 2007; da Costa et al., 2021). This is the case for the Loire estuary, where REE concentrations in abiotic compartments have already been characterized (Lortholarie, 2021). The Loire estuary drains the largest watershed of France, consequently it is under strong contaminant pressures due to anthropogenic activities (high population density, agricultural and industrial activities). The reported REE values were from 112.5 to 199.0 μg/g dw in the sediment (Thibault de Chanvalon et al., 2016; Lortholarie, 2021), from 51 to 489 μg/g dw in the suspended particulate matter (Thibault de Chanvalon et al., 2016; Lortholarie, 2021) and from 234 to 1,140 ng/L in the dissolved phase with a Gd positive anomaly (Lortholarie, 2021). The potential transfers from abiotic compartments to biota are poorly understood and appeared relevant to investigate in aquatic systems, regarding the global increase in the uses and discharges of these critical elements.

Many studies have already demonstrated a bioaccumulation of REEs after laboratory exposures, for example in fish (Qiang et al., 1994; Cardon et al., 2020), in bivalves (Perrat et al., 2017; Freitas et al., 2020; Lachaux et al., 2023) and in daphnia (Cardon et al., 2019). Some of them highlighted variations of the accumulation depending on the exposure dose (Freitas et al., 2020) or on the studied organ (Cardon et al., 2020), as well as variations of the subcellular distribution of REEs depending on the studied species (Cardon et al., 2019). REE potential toxic effects were also investigated by acute and chronic toxicity tests to estimate LC50 and EC50 in cnidarians (Blaise et al., 2018), daphnia (Barry and Meehan, 2000) or echinoderms (Gravina et al., 2018). Other works about REE toxicity in fish and bivalves (Perrat et al., 2017; Hanana et al., 2018; Zhao and Liu, 2018; Cardon et al., 2019; Freitas et al., 2020) investigated various effects related to growth rate, energy reserves, metabolism, detoxification processes, oxidative stress/antioxidant responses. Regarding studies on aquatic organisms from the field, REE bioaccumulation was reported in fish (Mayfield and Fairbrother, 2015; Yang et al., 2016; Li et al., 2016), turtles (Censi et al., 2013) and bivalves (Merschel and Bau, 2015; Wang et al., 2019; Briant et al., 2021; Figueiredo et al., 2022) but only few studies have investigated the fate of REEs in the entire ecosystem (Amyot et al., 2017; MacMillan et al., 2017; Wang et al., 2019; Santos et al., 2023). As REE concentrations in the environment tend to rise, field studies must be carried out to better understand the fate of REEs at the ecosystem level and, especially in food networks to (i) provide information on the accumulation by species according to their trophic position, their lifestyle and their role in the ecosystem; (ii) identify the most accumulative species; (iii) understand the transfers of REEs from abiotic to biotic compartments; (iv) acquire data to better monitor the REE enrichments in biota based on anthropogenic contributions and (v) assess the ecotoxicological risk of REEs.

This study aims to investigate the fate of REEs along the food web of the Loire estuary related to the abiotic compartment contamination. Total concentrations as well as individual contribution of each REE were evaluated in a wide variety of species representative of different trophic levels estimated by stable isotope analysis. Tissue-specific bioaccumulation was further examined for the vertebrate phylum. The anthropogenic origin of bioaccumulated REEs was also investigated using normalization and anomaly calculation methods.

2. Material and methods

2.1. Study area and sample collection

The Loire estuary extends for 97 km from Ancenis to the outside limit of Saint Nazaire and receives effluents from the largest watershed in France (118,000 km^2). It is subjected to strong anthropogenic pressure due to the high density of population gathered in two main cities: the Nantes metropolis (about 650,000 habitants) and Saint Nazaire city (about 70,000 habitants). The high industrialization of the area as well as the large agriculture activity make the Loire estuary a study area of particular interest for environmental issues.

Sampling sites were divided in 5 areas corresponding to Cordemais, Donges, Mindin, Saint Nazaire and Offshore (Fig. 1). They were selected to represent REE sources potentially different in terms of quantity, and quality as well, such as medical, agricultural or industrial uses. Cordemais is a small town of 3,600 inhabitants with a coal thermal power

station. Donges is a bigger town (7,700 inhabitants) with the second most important refinery of France. Mindin and St Nazaire areas are subjected to higher industrial activities, with an important harbor Shipyard and a WWTP. These sites are therefore impacted by REE releases through their uses in oil catalytic cracking, metallurgic alloys, permanent magnets or nuclear medicine. Finally, the Offshore zone is considered as the least exposed to anthropogenic inputs due to its position away from the coastline.

During April 2021, several species representative of different levels of the estuary food web were sampled in these locations: 8 vertebrates (*Trisopterus luscus*, $n = 9$; *Osmerus eperlanus*, $n = 3$; *Platichthys flesus*, $n = 16$; *Dicentrarchus labrax*, $n = 11$; *Chelon ramada*, $n = 12$; *Solea solea*, $n = 13$; *Anguilla anguilla*, $n = 4$; *Sprattus sprattus*, n = 9), 2 crustaceans (*Crangon crangon*, $n = 61$; *Palaemon longirostris*, $n = 51$), 2 mollusks (*Scrobicularia plana*, $n = 25$; *Limecola balthica*, n = 4), 3 annelids (*Nephtys hombergii*, n = 4; *Nereis diversicolor*, $n = 43$; *Heteromastus filiformis*), 4 algae (*Fucus vesiculosus*, n = 1; *Fucus spiralis*, n = 1; *Ulva lactuca*, n = 1; *Ulva intestinalis*, n = 1) and *Haploops sp.* tubes (Table S1, Fig. 1). *Haploops sp.* are small crustaceans living in sediment constituted tubes. As tubes and organisms were not separated for REE analysis, concentrations are mainly representatives of sediment levels, so they were not included in the crustacean phylum. The fish and shrimps were collected using a trawl. Mollusks, annelids, as well as *Haploops sp.* tubes, were sampled in the subtidal sediment (1 to 15 m depth and 20 to 23 m depth, respectively) using sampling buckets, whereas algae were manually collected during low tide in the intertidal zone. Due to a lack of sample mass for certain species, a complementary sampling was carried out during September 2022 in the subtidal sediment (1 to 15 m depth) of Cordemais and Donges, allowing the collection of additional individuals of *N. diversicolor* needed for stable isotope analysis. This second sampling also allowed the collection of another crustacean species, *i.e. Corophium volutator* ($n = 121$) (Table S1).

2.2. Sample preparation

All fish, *C. crangon* and *P. longirostris* were frozen at −20 °C onboard and transferred to the laboratory. Mollusks, annelids and *C. volutator* were transported alive to the lab in tanks with sediment and water from the sampling site. They were then manually sorted to be depurated for 48 h in artificial seawater, at the salinity and temperature of the site, before being frozen at −20 °C. Algae were identified in the lab and kept at −20 °C. Before freezing, all organisms were individually rinsed with deionized water, measured and weighed. Their habitat and food habit were recorded and are presented in Supplementary Material (Table S2). Fish were dissected to separately analyze muscle, gonads and the rest of the organism. Crustaceans, as well as *H. filiformis*, were grouped in several pools of individuals to reach the biomass required for chemical analysis. The whole soft tissues of the other species were individually used for analysis. Tissue samples were weighed, frozen, freeze-dried and grinded to obtain homogeneous samples.

Fish tissue samples (except gonads and *S. sprattus*) went through a preliminary step of calcination to concentrate the samples: 1 g dw of each tissue was carbonized in a muffle furnace (Nabertherm LE) for 1 h at 300 °C and 2 h at 500 °C. Then, the digestion step was performed on either ash from calcination or dry samples. Briefly, 200 mg were predigested at room temperature in Teflon vessels with a mix of HNO_3 65 % / HCl 37 % (9:1, v/v). After 1 h, samples were mineralized in a microwave oven (Multiwave GO Plus, Anton Paar) with the following program: 5 min reaching 100 °C maintained during 10 min and 15 min reaching 170 °C maintained during 35 min. Digested solutions were then transferred into Pyrex tubes to be evaporated to dryness on a hot-plate at 130 °C. When the dry weights were lower than 60 mg, samples were directly digested in Pyrex tubes placed on a hot-plate at 90 °C until full mineralization instead of being microwaved. Samples were then resuspended in 1.8 mL of HNO_3 2 %, vortexed, sonicated for 10 min and centrifuged (3 rpm) for 5 min. The supernatants were finally diluted and analyzed.

To assess the accuracy of the analytical procedure, all samples were treated in triplicates when possible. In parallel to samples, procedural blanks were processed, as well as an international certified reference material (CRM, BCR® - 668, mussel tissue). All the materials used during field and laboratory work were previously washed with detergent and water. Then, they were bathed in acid (HNO_3 10 %) and rinsed with ultrapure water (Milli-Q, Millipore).

To perform stable isotope analysis, about 200 mg of grinded dry tissue of fish muscle or whole soft tissue of other species were aliquoted and precisely weighed in pewter capsules for further analysis.

2.3. Rare earth element analysis by ICP-MS

REE concentrations were determined using an inductively coupled plasma mass spectrometer (ICP-MS, NexION 300×, PerkinElmer) equipped with an autosampler S10 (PerkinElmer) and Ar as collision gas. The following REE isotopes were selected: ^{89}Y, ^{139}La, ^{140}Ce, ^{141}Pr, ^{142}Nd, ^{147}Sm, ^{153}Eu, ^{155}Gd, ^{159}Tb, ^{163}Dy, ^{165}Ho, ^{166}Er, ^{169}Tm, ^{171}Yb and ^{175}Lu. External calibrations using multi-elemental standard solutions (NexION setup solution, PerkinElmer) were performed at the beginning of each analytical session. All samples, blanks, standard and CRM were diluted with HNO_3 2 % and rhenium (^{187}Re) was used as internal standard at a concentration of 1 µg/L in each sample. As some samples had a high viscosity, instrumental blanks (2 % HNO_3) were inserted between each sample to help the rinsing of the machine pipes. For quality controls, standard solutions containing 1 and 5 µg/L of REEs were running on the ICP-MS every 5 samples. REE concentrations in blanks were subtracted from sample concentrations. Then, they were corrected according to the recovery of REEs in the CRM (Table S3). The limits of detection (LOD) and of quantification (LOQ) were determined for each REE as following: LOD = [(standard deviation of y-intercept / slope) * 3.3] and LOQ = LOD * 3 (Table S3). The results from the samples were compared to these limits. The concentrations were considered as equal to 0 or equal to the LOD when the results were lower than the LOD and the LOQ respectively.

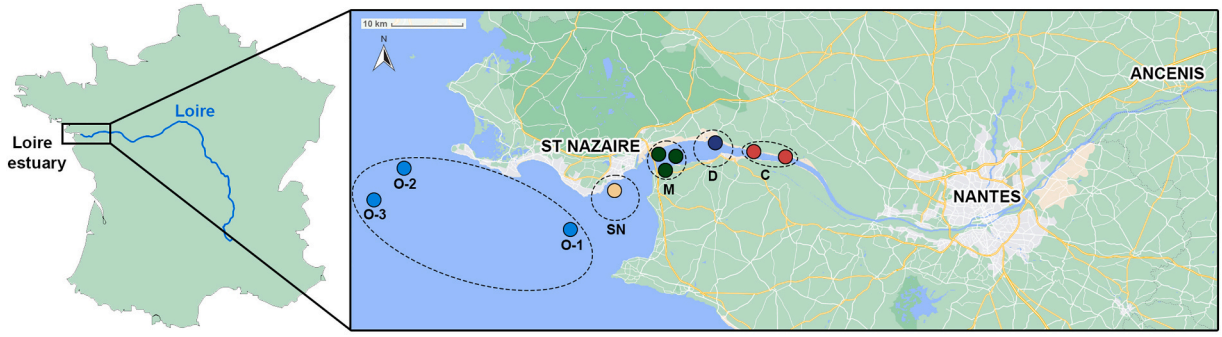

Fig. 1. Sampling sites of the Loire estuary. C: Cordemais, D: Donges, M: Mindin, SN: Saint Nazaire, O-1: Offshore-1, O-2: Offshore-2 and O-3: Offshore-3.

2.4. $\delta^{13}C$ and $\delta^{15}N$ analysis

Stable isotopic composition of C and N ($\delta^{13}C$ and $\delta^{15}N$) was analyzed in the muscle of fish, the soft tissue of mollusks and the whole organism of crustaceans, annelids and algae by the IPSiM (Institut des Sciences des Plantes de Montpellier, France) using an isotope ratio mass spectrometer (IRMS, isoprime precisION, Elementar) coupled with an elemental autoanalyzer (EA, vario PYRO cube, Elementar). Isoleucine (calibrated with IAEA-CH-6 and IAEA-NO-3) was used as internal standard and was run every 24 samples. Isotopic data are expressed using the usual delta (δ) notation with a per mil deviation (‰) from international reference materials (Vienna Pee Dee belemnite and atmospheric N_2 for $\delta^{13}C$ and $\delta^{15}N$, respectively). Concerning *N. diversicolor* and *C. volutator*, the analysis was performed on organisms collected in September 2022.

2.5. Data processing

REE concentrations are presented in nanograms or micrograms per gram of sample dry weight (ng or μg/g dw) and total REE concentrations (ΣREEs) were calculated as the sum of the individual REEs. Median and median absolute deviation (MAD) were used to describe the data (REE concentrations and anomaly values). Individual REE contributions were calculated as a mean percentage (%) for each REE. The REEs from La to Nd, from Sm to Gd and from Tb to Lu in addition to Y corresponded to LREEs, MREEs and HREEs, respectively. Pm was excluded because it is radioactive and not naturally present in the environment.

In order to visualize anomalies, REE concentrations were normalized to Post Archean Australian Shale (PAAS) (Pourmand et al., 2012; Rétif et al., 2023). Only elements quantified in more than 30 % of the total samples of each studied species were considered on the REE spectra (Tables S4 and S5). Anomalies were calculated by estimating the geogenic background concentration of the studied elements by modeling the shape of the normalized REE pattern, using a third-order polynomial fit, excluding anomalous elements (Möller et al., 2002, 2003; Hatje et al., 2016). Ce and Eu were excluded of the models because of their redox sensitivity, as well as Gd, Tb, Tm and Lu, since they seemed anomalous in the drawn REE patterns. Anomalies were calculated for Eu, Gd, Tb and Lu using the Eq. (1):

$$REE_N / REE_N^{*} = REE_N / \left(ax^3 + bx^2 + cx + d\right) \quad (1)$$

where REE_N is the PAAS-normalized studied REE concentration and REE_N* is the geogenic background concentration calculated by solving each fitted third-order polynomial of a, b, c and d parameters for x = position of the studied REE (7, 8, 9 and 15 for Eu, Gd, Tb and Lu, respectively) (da Costa et al., 2021). Values higher than 1 indicate positive anomalies and values lower than 1 indicate negative anomalies. To compare the results obtained from the biota to the abiotic compartments and assess the potential REE transfers, the spectra of abiotic compartments (Lortholarie, 2021) were added in the REE-pattern figures.

The trophic transfer of REEs was characterized by estimating the trophic magnification slope (TMS) which is an indicator of the biomagnification potential of contaminants. It is based on the studied contaminant concentrations and the stable nitrogen isotope values ($\delta^{15}N$) which are often used to characterize the trophic level of organisms. An increased $\delta^{15}N$ value indicates a higher trophic level within a food web. Thus, the TMS corresponds to the slope (b) of the linear regression of $\log_{10}[\Sigma REE]$ related to $\delta^{15}N$ (Eq. (2)).

$$log_{10}[\Sigma REE] = \delta^{15}N(b) + a \quad (2)$$

A positive TMS value indicates biomagnification in the food web whereas a negative value highlights a trophic dilution.

2.6. Statistical analysis

The statistical analysis was carried out using Rstudio. The normality of the data was investigated using Shapiro-Wilk tests and, as most of the data were not meeting the normality requirement, non-parametric tests were performed. For multiple groups comparison, Kruskal-Wallis tests were used followed by post-hoc multiple comparison Nemenyi tests, in case of significant differences between the studied groups. Wilcoxon's tests were performed for pairwise comparison, as well as to verify the presence of anomalies (values $\neq 1$). Linear regression model analysis was done using the 'lm' function and was tested with a Pearson correlation test. The significance level for all statistical tests was set at *p-value* ≤ 0.05.

3. Results and discussion

3.1. REEs in the food web

3.1.1. REE concentrations

REE concentrations measured in several species of the Loire estuary food web highlighted the following accumulation order: *Haploops sp.* tubes > algae > mollusks > annelids > crustaceans > vertebrates (Fig. 2, Table S6) which is comparable to the other studies investigating the REE concentrations in a wide range of species (MacMillan et al., 2017; Squadrone et al., 2019; Wang et al., 2019; Marginson et al., 2023; Santos et al., 2023). This observation can be due to different accumulation of REEs by the various species, depending on their habitat and food habit. Benthic organisms, as well as primary producers, planktivorous, suspensors, detritivores or deposit-feeders might be more exposed to REEs due to their direct contact with sediments, where REEs tend to be accumulated (Censi et al., 2007; Amyot et al., 2017).

The highest REE concentrations were measured in the *Haploops sp.* tubes (141.1 ± 4.7 μg/g dw) which mostly correspond to sediments than organisms, as explained in the material and methods section (Fig. 2). These results are consistent with previous results recording REE concentrations reaching 195 to 199 μg/g dw in the Loire estuary sediments (Thibault de Chanvalon et al., 2016). It is also comparable to many other studies focusing on REEs in sediments at: the Marabasco estuary, Mexico (27.5–157.3 μg/g dw), the Bohai Bay, China (97.6–202.0 μg/g dw), the Tagus estuary, Portugal (18–210 μg/g dw), the Jaguaripe estuary (202–220 μg/g dw) and the Subae estuary (25.6–198.0 μg/g dw), Brazil (Marmolejo-Rodríguez et al., 2007; Zhang et al., 2014; Brito et al., 2018; de Freitas et al., 2021; Santos et al., 2023).

High REE levels were recorded in algae compared to the other studied species (Fig. 2) and the differences were marked between their genus with lower concentrations in brown algae *Fucus sp.* (1.51–3.50 μg/g dw) compared to green algae *Ulva sp.* (19.27–34.45 μg/g dw). These values are in the same order of magnitude than others found in several studies carried out by Squadrone et al. (2017, 2018, 2019) on both green and brown algae (2.09–27.00 μg/g dw), as well as in the brown algae *Alaria sp.* (5.22–25.80 μg/g dw) from eastern Canadian subarctic (Marginson et al., 2023). Higher values than those recorded in the present study (*Fucus sp.*) were reported in the brown algae *Padina sp.* (8.4–62.2 μg/g dw) from the east coast of Peninsular Malaysia (Mashitah et al., 2012). Lower contents were also measured in other brown algae (148.1–534.8 ng/g dw) collected in Japan coasts (Sakamoto et al., 2008) and in *Ulva sp.* (548 ng/g dw) from Aburatsubowan Bay, Japan (Fu et al., 2000). Fu et al. (2000) also showed lower values in brown algae (50–121 ng/g dw) compared to green algae (215–548 ng/g dw). These results highlight the capacity of seaweeds to accumulate REEs, especially green algae (*Ulva sp.*) that could be used as bioindicators. Additionally, these organisms play an important role in the REE transfer to other organisms of the ecosystem, such as omnivorous, deposit feeders, grazers or detritivores.

The two studied mollusks had similar REE concentrations (9.91 ± 0.38 μg/g dw in *L. balthica* to 11.98 ± 5.48 μg/g dw in *S. plana*, Fig. 2) that are close to REE values reported in various bivalve species

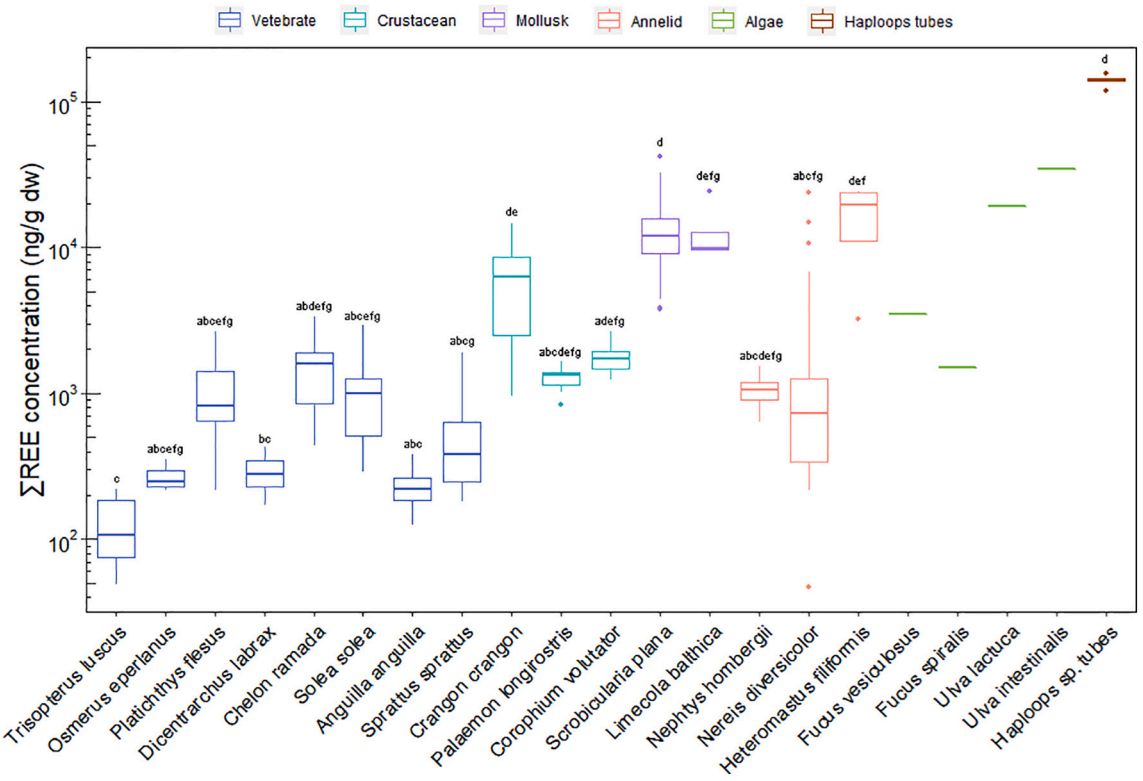

Fig. 2. Median concentrations of ΣREEs (log_{10}-scaled axis, ng/g dw) in the organisms of the Loire estuary food web colored by phylum and organized by decreasing trophic level. Different letters represent significant differences (Kruskal-Wallis test, *p-value* ≤ 0.05) between studied species for which $n > 2$. Lower and upper margins of boxes show 1st and 3rd quartiles, whiskers represent maximum and minimum values, the median is defined by the bold line and outliers are drawn as individual points.

(1.28–6.68 μg/g dw) of the Subae estuary (Santos et al., 2023), as well as in mussels or oysters from the eastern Canadian arctic (3.71–6.23 μg/g dw) and subarctic (5.91–15.13 μg/g dw), the French metropolitan coasts (0.002–10.940 μg/g dw) and the Portuguese (0.17–9.69 μg/g dw) ones (MacMillan et al., 2017; Briant et al., 2021; Figueiredo et al., 2022; Marginson et al., 2023). They were however higher than reported values in gastropods (0.03–1.48 μg/g dw) from the Nansha sea (Li et al., 2016), in bivalves from Tokyo (1.15–3.48 μg/g dw) and Mulan (389.7–496.2 ng/g dw) Bays (Akagi and Edanami, 2017; Wang et al., 2019) and from Northwestern Italy (110–140 ng/g dw) (Squadrone et al., 2019). Lower REE concentrations (1.1–454.0 ng/g dw) were also described in *Corbicula fluminea* from the Jiangxi Province (Wang et al., 2022). Bivalves have been widely used for years now as bioindicators of aquatic pollution as they tend to accumulate contaminants in their tissues, such as trace metal elements, including REEs (Bonnail et al., 2017; Perrat et al., 2017; Figueiredo et al., 2022). Their filter-feeding mode, as well as their habitat at the water-sediment interface, make these organisms particularly exposed to contaminants both directly (dissolved forms) and trophically (adsorbed on ingested nutrient particles) (Fournier et al., 2005) and explains the high recorded REE levels.

Among annelids, *H. filiformis* stood out with much higher concentrations (Fig. 2), up to 19.99 ± 5.52 μg/g dw, compared to *N. hombergii* and *N. diversicolor* (1055.6 ± 332.2 and 717.5 ± 626.1 ng/g dw, respectively). It could be explained by the depuration process that was not complete for *H. filiformis* due to the difficulty of keeping the organisms alive during that step. This is consistent with the comparable concentrations measured in non-depurated polychaeta (24.15 μg/g dw) found in a previous study (Santos et al., 2023). It also highlights the importance of the depuration process in assessing REE concentrations within organisms (Amyot et al., 2017; Benaltabet et al., 2021). In fact, although these organisms live buried in the sediment, compartment with high REE concentrations, they do not seem to accumulate REEs in their tissue. REE quantification levels of both depurated species (*N. hombergii* and *N. diversicolor)* were often under the quantification limit of the method (particularly HREEs, Table S4), demonstrating that higher recorded REE concentrations in *H. filiformis* could be mostly due to remaining sediments in the organism' guts.

Crustacean phylum showed variations depending on the studied species with higher values in *C. crangon* (6.30 ± 5.34 μg/g dw) compared to *P. longirostris* (1.35 ± 0.10 μg/g dw) and *C. volutator* (1.74 ± 0.41 μg/g dw) (Fig. 2). These concentrations are similar to those recorded in *Litopenaeus sp.* from Brazil (5.50 μg/g dw in internal organs and 422 ng/g dw in muscle) but particularly higher than those presented in the *Penceus penicillatus* shrimp (36.4 ng/g dw) from China (Santos et al., 2023; Wang et al., 2019). These relatively high values could be explained by the benthic habitat of shrimps but also by their food habit, exposing them to REEs. A study of Marchand (1981) on the food diet of *C. crangon* and *P. longirostris* demonstrated that although they largely consume annelids and copepods, they also ingest high quantity of sediment, allowing the grinding of food and the intake of microorganisms.

The lowest REE concentrations were measured in the vertebrate phylum. Concentrations ranged from 106.5 ± 52.3 ng/g dw in *T. luscus* to 1610.0 ± 704.9 ng/g dw in *C. ramada* (Fig. 2). Results are close to values measured in whole body of freshwater fish by Mayfield and Fairbrother (2015) in Washington state, USA (14–3000 ng/g dw) and by Amyot et al. (2017) in temperate lakes of Quebec, Canada (110–450 ng/g dw). Lower values were reported in fish from the Nansha sea (Li et al., 2016) and from in the Maluan Bay (Wang et al., 2019) in China, with respective values reaching 4.1 to 44.7 ng/g dw and 5.4 to 14.0 ng/g dw. Results showed greater concentrations in demersal species, as well as in pleuronectiforms species (*P. flesus*, *S. solea*) compared to pelagic ones (*T. luscus*, *O. eperlanus*, *S. sprattus*) (Fig. 2, Table S2). This indicates the

important role of sediment in the direct REE exposure for fish. In addition, higher REE values were reported in plankton-feeding species (*P. flesus*, *C. ramada*, *S. sprattus*) compared to exclusive carnivorous/piscivorous (*T. luscus*, *O. eperlanus*, *D. labrax*, *A. anguilla*) (Fig. 2, Table S2), since plankton is known to particularly accumulate REEs (Amyot et al., 2017; MacMillan et al., 2017; Santos et al., 2023). These observations demonstrate the food habits as of major influence in the REE transfer to organisms.

As an overall, several factors, such as the geochemical background, the REE anthropogenic sources, the REE bioavailability depending on the physiochemical environmental conditions or the variability of uptake and elimination processes depending on the species, could explain the differences between the reported REE concentrations in this study and the others.

Regarding the spatial variations, the comparison of the different sampling sites highlighted a tendency of higher REE concentrations at Mindin than at Cordemais which was significant only for *P. flesus*. The REE concentrations were also significantly higher at Donges than at Mindin for *S. plana* (Fig. S1, Table S7). These different concentrations could be explained by higher industrial activities near Mindin compared to Cordemais. Mindin is characterized by the proximity of an important harbor, as well as a shipyard and a WWTP. The Donges refinery could also explain the higher values reported in *S. plana* from Donges compared to Mindin as REEs are used in the oil catalytic cracking.

3.1.2. REE distribution

The individual contribution of REEs was also investigated (Fig. 3, Table S8). The distribution patterns were similar for most of the studied species with the highest contribution of LREEs, then HREEs and MREEs. The LREEs corresponded to 48.3 to 87.3 % of the total REE concentrations with a predominance of Ce. The HREEs reached 5.5 to 23.2 %, with the highest percentage for Y and the MREEs were between 4.3 and 33.2 %, mainly due to the Gd contribution. These observations are comparable to many other studies on various organisms, demonstrating higher contribution/concentrations of LREEs compared to HREEs and/or MREEs (MacMillan et al., 2017; Squadrone et al., 2019) with a predominance of Ce (Wang et al., 2019; Lortholarie et al., 2021; Marginson et al., 2023; Labassa et al., 2023). The presented results are also consistent with the known abundance of the different classes of REEs in the earth's crust. Indeed, LREEs are generally more abundant than MREEs and HREEs, Ce being the most abundant REE in the environment (Christie et al., 1998; Bru et al., 2015). However, the possible higher bioavailability of LREEs, including Ce, could also be a reason for the high recorded percentages of this element (22.0–43.2 %) in the studied organisms. Only *N. hombergii*, *P. longirostris* and *Haploops sp.* tubes showed a different distribution pattern, *i.e.* LREEs > MREEs > HREEs. For *N. hombergii*, this difference was explained by high percentages of MREEs, up to 33.2 %, including 18.8 % and 14.2 % of Gd and Sm respectively, as well as low percentages of LREEs, decreasing to 48.3 %, with only 22 % of Ce contribution compared to 30.7 to 43.2 % in other species. The low quantification of HREEs (except Y) compared to LREEs and MREEs in this species (Table S4) could also be an explanation for the diverging reported distribution pattern. For *P. longirostris*, the MREE contribution (10.6 %) was quite the same as the HREE contribution (9.6 %). Finally, no Y contribution was recorded for *Haploops sp.* tubes, as this element was not analyzed for these samples, explaining the low contribution of HREEs leading to a pattern diverging from the others.

3.1.3. Eu, Gd, Tb and Lu anomalies

The presence of anomalies was examined by normalizing REE concentrations to PAAS (Fig. 4) and REE patterns of abiotic compartments were added to the figure for comparison. The PAAS-normalized patterns of vertebrates showed Eu, Gd, Tb and Lu positive anomalies, also noticeable for crustaceans (Fig. 4A,B). Mollusks, annelids, *Haploops sp.*

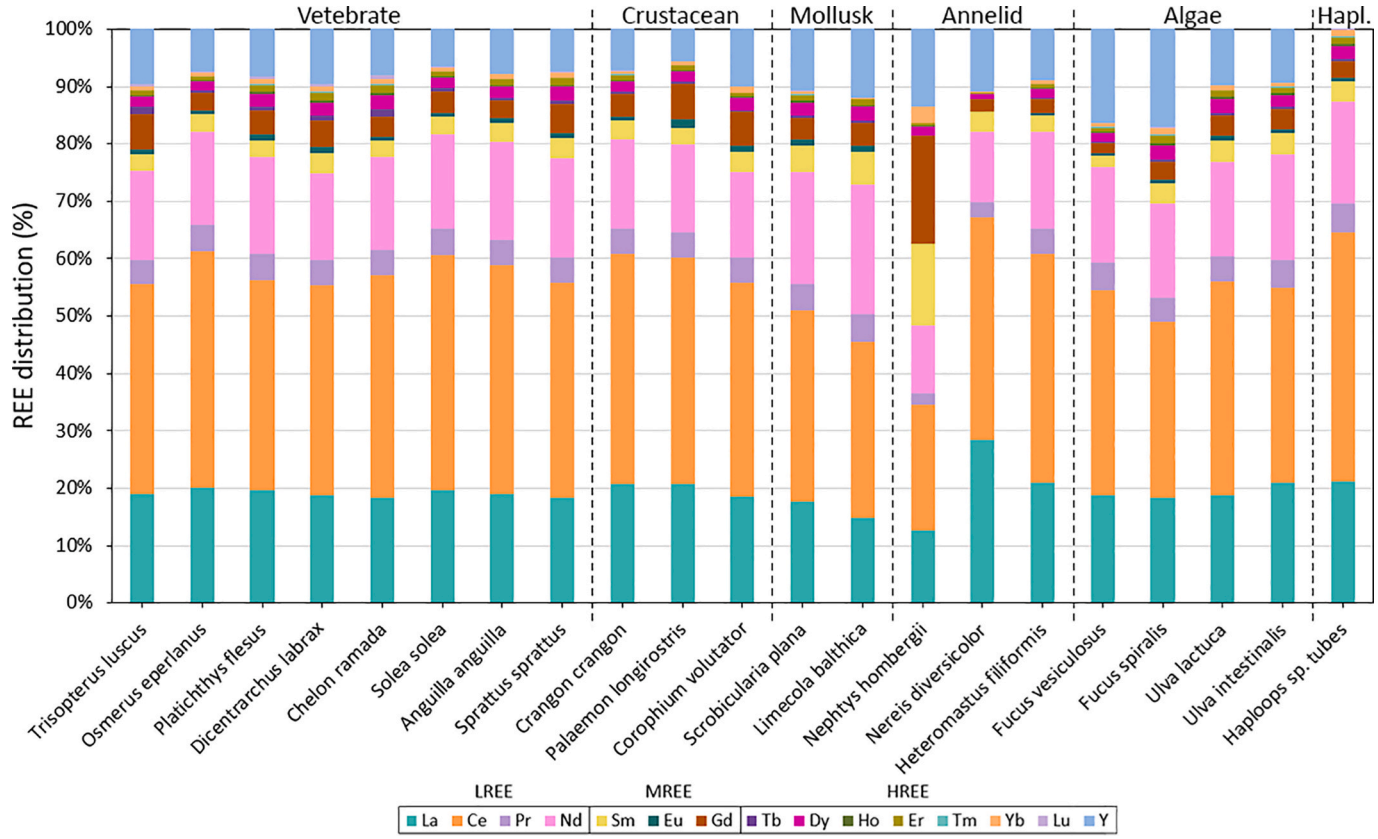

Fig. 3. REE distribution (%) in the organisms of the Loire estuary food web organized by decreasing trophic level. Hapl.: haploops tubes.

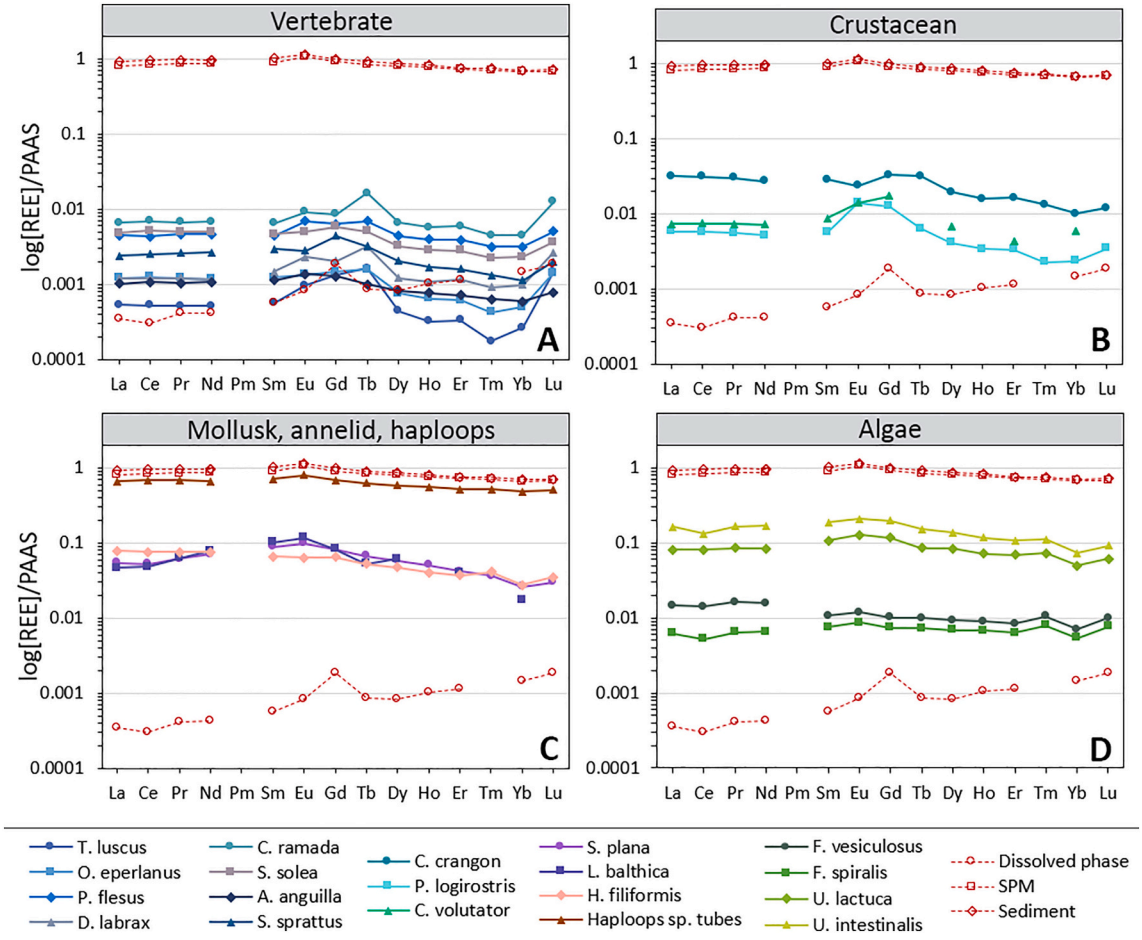

Fig. 4. PAAS-normalized REE patterns for the vertebrates (A), crustaceans (B), mollusks, annelids, haploops tubes (C) and algae (D) along with abiotic compartment patterns (dissolved phase, suspended particulate matter (SPM) and sediment derived from Lortholarie, 2021) of the Loire estuary. *N. hombergii* and *N. diversicolor* patterns are not represented due to the low quantification of REEs in these species. Post-Archean Australian Shale normalization was performed using Pourmand et al. (2012) dataset.

tubes and algae patterns were relatively flat (Fig. 4C,D). Eu, Gd, Tb and Lu anomalies were calculated for each species (Fig. 5, Table S6).

Reported Eu anomalies ranged from 0.88 to 2.45, with values significantly higher than 1 for *P. flesus*, *P. longirostris*, *C. volutator* and *L. balthica* (Fig. 5A). The vertebrate values ranged from 1.11 ± 0.50 for *S. sprattus* to 1.87 ± 1.09 for *D. labrax* and the highest recorded values were for crustaceans with *C. volutator* (2.10 ± 0.23) and *P. longirostris* (2.45 ± 0.27). Mollusks, *H. filiformis*, algae and *Haploops sp.* tubes showed lower values from 0.89 for *F. vesiculosus* to 1.48 for *U. lactuca*.

Gd anomalies were ranging from 0.83 to 2.55 and were significantly higher than 1 for *T. luscus, D. labrax*, *P. longirostris and C. volutator* (Fig. 5B). Similarly to Eu, the calculated anomaly values were higher in vertebrates (from 1.19 ± 0.5 for *O. eperlanus* to 2.35 ± 1.31 for *T. luscus*) and crustaceans, especially *C. volutator* and *P. longirostris* (2.44 ± 0.32 and 2.55 ± 0.51, respectively). On the contrary, the values were lower in mollusks, *H. filiformis*, algae and *Haploops sp.* tubes (0.83 for *F. vesiculosus* to 1.35 for *U. lactuca*).

Tb anomalies were less homogenous among the studied species and ranged from 0.91 to 2.85 with values significantly higher than 1 for *T. luscus, C. ramada* and *S. solea* (Fig. 5C). Anomalies were also higher in vertebrates (1.03 ± 0.27 for *S. sprattus* to 2.85 ± 1.21 for *T. luscus*) and crustaceans (1.49 ± 0.21 in *P. longirostris* to 1.50 ± 1.16 in *C. crangon*) compared to other phyla. The median values were higher than 2 for three species, *i.e. T. luscus* (2.85 ± 1.21), *D. labrax* (2.46 ± 2.18) and *C. ramada* (2.29 ± 1.00). Mollusks, *H. filiformis*, algae and *Haploops sp.* tubes anomaly values ranged from 0.91 (*F. vesiculosus)* to 1.57 ± 0.18 (*H. filiformis*).

The highest anomaly values were recorded for Lu (1.13 to 10.76) and led to median values above 1 for all the species, with statistical significance only for 7 of them, *i.e. T. luscus*, *P. flesus*, *D. labrax*, *C. ramada*, *S. solea*, *P. longirostris*, *S. plana* (Fig. 5D). *T. luscus* clearly stood out with a median value of 10.76 ± 3.07, much higher than all other studied species with values reaching 1.13 ± 0.21 for *Haploops sp.* tubes, 1.33 to 1.79 for algae, 2.32 ± 0.19 for *H. filiformis*, 2.74 ± 0.79 for *S. plana*, 2.00 ± 0.48 to 2.36 ± 0.51 for crustaceans and finally 1.57 ± 0.70 to 3.48 ± 3.18 for other vertebrates.

The Gd anomalies observed in biota are consistent with anomalies found in the dissolved phase of the Loire estuary (Fig. 4, Lortholarie, 2021) and are comparable to various studies reporting the same anomaly in rivers (Bau and Dulski, 1996), estuaries (da Costa et al., 2021), seawater (de Baar et al., 1985) or bivalves (Pereto et al., 2020). Eu anomalies are often reported in the water column (Censi et al., 2004; MacMillan et al., 2017; Pignotti et al., 2017) and is also noticeable in the dissolved phase REE-pattern of the Loire estuary (Fig. 4). It is mostly due to the reduction of Eu (III) to Eu (II), which is more soluble (Goldstein and Jacobsen, 1988), and might therefore be more bioavailable to organisms. Concerning Tb and Lu anomalies, few studies reported anomalies for these two elements (de Baar et al., 1985). In the Loire estuary, no Tb or Lu anomalies are noticeable in abiotic compartment REE-patterns (sediment, suspended particulate matter or dissolved phase), although a gradual enrichment in HREEs can be observed in the dissolved phase (Fig. 4). The latter is not observed in the pattern of the

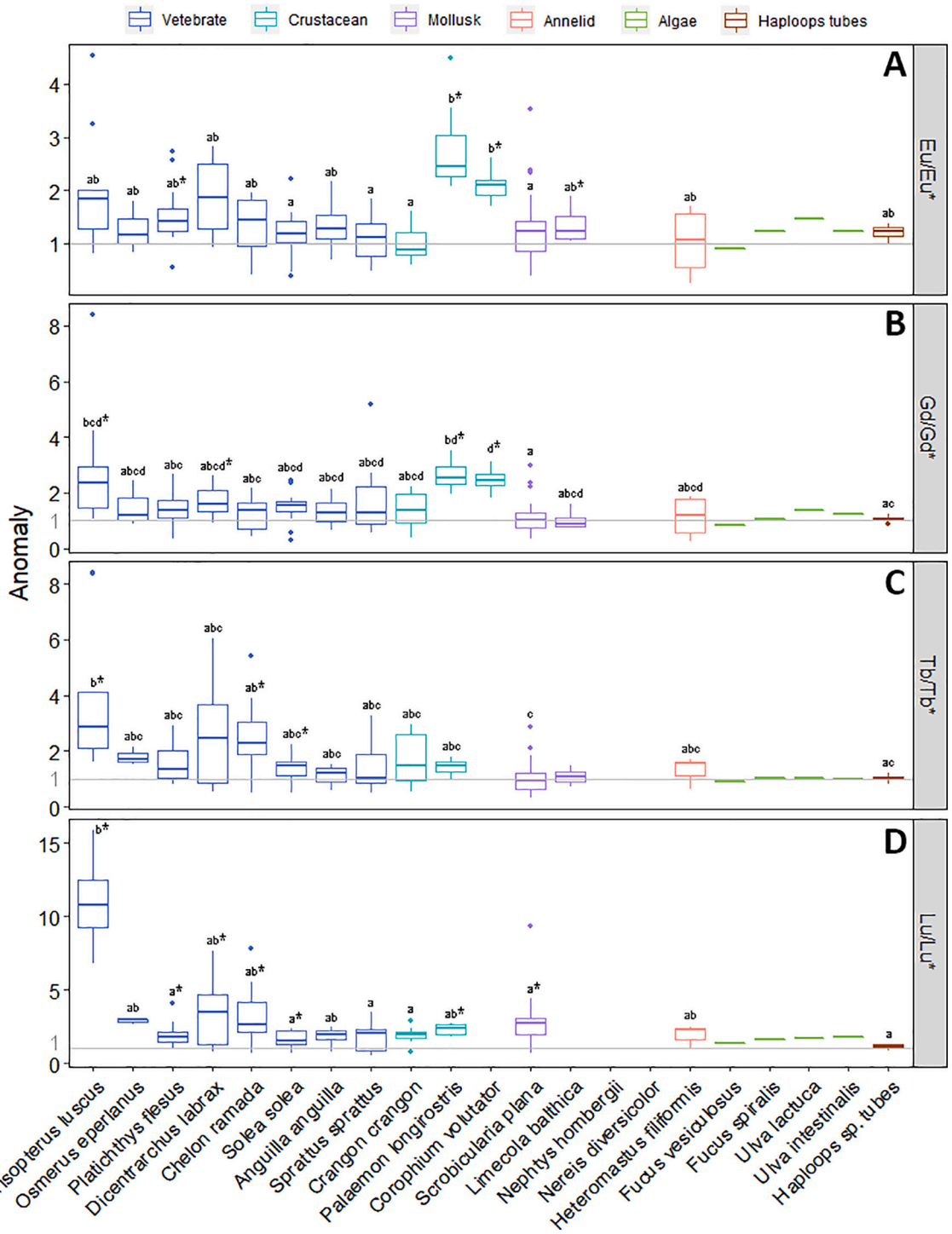

Fig. 5. Eu (A), Gd (B), Tb (C) and Lu (D) anomalies in the organisms of the Loire estuary food web colored by phylum and organized by decreasing trophic level. Different letters represent significant differences (Kruskal-Wallis test, *p-value* ≤ 0.05) between studied species for which n > 2. Values significantly higher than 1 (Wilcoxon test, *p-value* ≤ 0.05) are denoted by superscript "*". Lower and upper margins of boxes show 1st and 3rd quartiles, whiskers represent maximum and minimum values, the median is defined by the bold line and outliers are drawn as individual points.

studied species, apart from enrichments in Tb and Lu, underlining the involvement of mechanisms other than bioavailability in the REE bioconcentration. Although the vertebrates seem to be less accumulating REEs, they show the most significant anomaly values. As Gd and Eu anomalies are mostly reported in the dissolved phase, the studied fish species, being either demersal or pelagic (Table S2), might be more exposed to these two REEs through the water column. In comparison, benthic organisms (like mollusks or annelids, Table S2), living in the sediment, are therefore mostly exposed to geogenic REEs. This is confirmed by the higher values of their relatively flat spectra, close to the one observed for sediments. The differences of REE accumulation among the studied species are thus relatively consistent with the REE distribution among the Loire estuary abiotic compartments. The water column's dissolved phase indeed showed globally lower REE concentrations than those measured in the suspended particulate matter or sediment (Fig. 4). Nevertheless, the dissolved concentrations in water

seems to be more impacted by anthropogenic inputs, with a Gd contamination that might be transferred to demersal or pelagic biota (Fig. 4). This, along with Eu reduction, could explain Gd and Eu anomalies reported in organisms, but considering Tb and Lu, it might involve other mechanisms. The bioaccumulation processes could differ from a species to another, as it was already demonstrated for Y (Cardon et al., 2019) or other metals like Cd (Le Croizier et al., 2019). It could also depend on the life stage or gender of the individuals, within a same species, as recently reported for REEs in *A. anguilla* (Lortholarie et al., 2021). These results demonstrate the important influence of species physiology in the uptake, the preferential internalization or the elimination of some metals/REEs, such as with Eu, Gd, Lu and Tb shown in the present study, mostly accumulated by vertebrates and crustaceans.

Some anthropogenic origins can also be considered to explain the recorded anomalies regarding the current uses of REEs. Eu is widely used in industry as phosphor for its fluorescent property, as well as in nuclear energy as neutron absorbers in nuclear reactor control rods (Bru et al., 2015). Chelate forms of Gd are extensively used as contrast agents during MRI (Blomqvist et al., 2022), reaching 22 to 66 tons of Gd used each year. Each examination requires 1.1 to 1.3 g of Gd^{3+} (Thomsen, 2017) and various studies have already linked the positive recorded anomalies in natural environments to anthropogenic uses of Gd (Kümmerer and Helmers, 2000; Rabiet et al., 2009; Verplanck et al., 2010). Tb is used as theragnostic radio-isotopes, especially four isotopes, *i.e.* ^{152}Tb and ^{155}Tb used for PET (positron emission tomography) and SPECT (single-photon emission computed tomography) imaging, along with ^{149}Tb and ^{161}Tb used for radiotherapy (Müller et al., 2018; Naskar and Lahiri, 2021). Concerning Lu, it is also widely used in radionuclide therapy, particularly in treatments for men with prostate cancer. The high affinity of ^{177}Lu with the prostate specific membrane antigen (PSMA, a receptor on the surface of prostate cancer cells) allows a better precision and quality of PET imaging, as well as targeted radionuclide therapy (Pillai and Knapp, 2015; Emmett et al., 2017). However, as ^{177}Lu disintegrates into hafnium (Hf) within 6 days, it might not be the main source for the reported Lu anomalies.

Site comparison highlighted a trend with higher values of Eu and Gd anomalies recorded at Mindin compared to Cordemais. The differences were significant only for *P. flesus* and *S. solea* considering Eu anomalies and for *P. flesus* considering Gd anomalies (Fig. S2, Table S7). These higher Eu and Gd contents in organisms from Mindin are consistent with the overall higher REE concentrations reported in the vertebrates from Mindin compared to Cordemais (Fig. S1). In addition to the potential REE sources higher in Mindin than Cordemais, Mindin is located in the polyhaline zone of the estuary whereas Cordemais is in the mesohaline zone. The REE agglomeration in sediment at high salinity (Tepe and Bau, 2016; Thibault de Chanvalon et al., 2016), as well as *P. flesus* and *S. solea* being demersal species particularly exposed to sediment, could explain the significant higher reported Eu and Gd anomalies in Mindin compared to Cordemais for these two species. However, this trend was not observable for Tb and Lu anomalies, depending on studied species displaying either similar values between the two sites or values higher at Cordemais than at Mindin (except for *P. flesus* and *C. crangon*). Additionally, Eu, Gd, Tb and Lu anomalies recorded at Donges were significantly higher compared to Mindin for *S. plana* (Fig. S2, Table S7) which is comparable to results previously presented for total REE concentrations (Fig. S1).

3.2. Bioaccumulation of REEs in fish tissues

3.2.1. REE concentrations

REE concentrations in the muscle and gonads of fish were also measured (Fig. 6, Table S9). Concentrations were distributed as follow: whole organism > gonads ≥ muscle for all studied species, except *O. eperlanus*. Muscle REE concentrations ranged from 21.10 ± 4.61 ng/g dw for *A. anguilla* to 264.0 ± 146.3 ng/g dw for *C. ramada*. In gonads, they ranged from 31.10 ± 2.18 ng/g dw for *O. eperlanus* to 135.5 ± 84.5 ng/g dw for *S. sprattus*. The results for *A. anguilla* muscle were comparable to those found in recent studies performed by Lortholarie et al. (2020, 2021) in the same species and the same study area, recording values from 2.9 to 12.6 ng/g dw in the muscle. Concerning the other fish species, the concentrations of *S. solea* muscle found in the present study (114.0 ± 90.7 ng/g dw) are greater than those recorded in the west Gironde mud patch area (4.38 ± 1.20 ng/g dw) (Labassa et al., 2023) which is a less industrialized area with a preserved natural balance. Several other studies showed the same range of REE concentrations measured in fish muscle, *e.g.* 23 to 460 ng/g dw in fish from Ligurian sea, Italy (Squadrone et al., 2019), 17.4 to 60.4 ng/g dw in fish species from the Subae estuary, Brazil (Santos et al., 2023), 76 to 191 ng/g dw in Baltic herring and European sardine from the Gdansk Bay and the Iberian Peninsula (Reindl and Falkowska, 2021) as well as 1 to 116 ng/g dw and 9 to 80 ng/g dw in fish from the eastern Canadian arctic and subarctic region respectively (MacMillan et al., 2017;

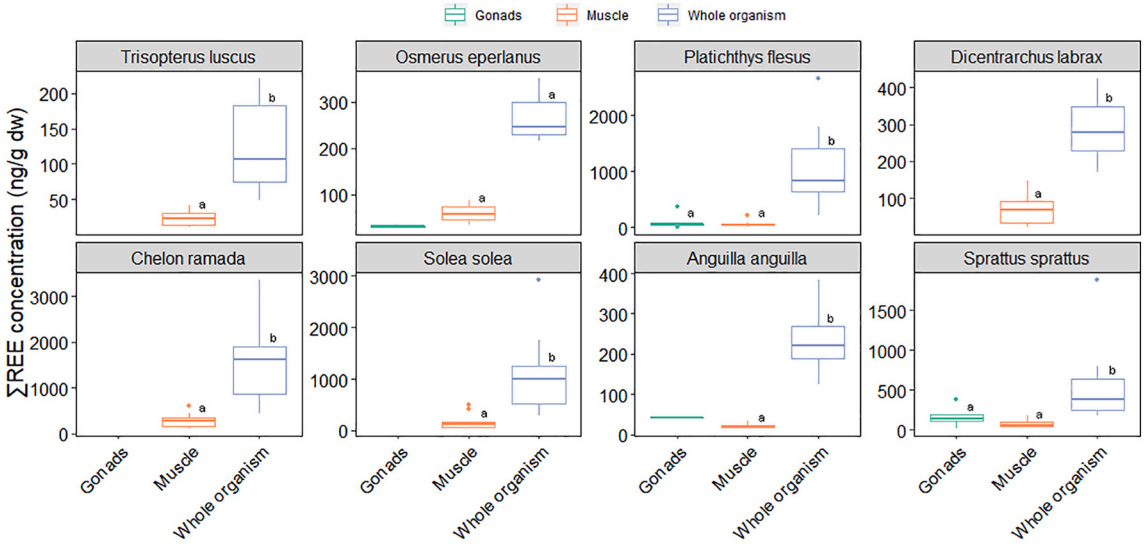

Fig. 6. Median concentrations of ΣREEs (ng/g dw) in the tissues of vertebrates from the Loire estuary food web. Different letters represent significant differences (Kruskal-Wallis or Wilcoxon test, *p-value* ≤ 0.05) between studied tissues (for which n > 2) within each species. Lower and upper margins of boxes show 1st and 3rd quartiles, whiskers represent maximum and minimum values, the median is defined by the bold line and outliers are drawn as individual points.

Marginson et al., 2023). Lower concentrations (3–10 ng/g dw) were reported in muscle of freshwater fish from temperate lakes of Quebec (Amyot et al., 2017). Concerning the gonads, recorded values of the present work are higher than other published results for *A. anguilla* (5.42–37.67 ng/g dw) from the same study site (Lortholarie et al., 2021).

These results are consistent with previous studies on fish showing higher concentrations in whole organism/internal organs compared to muscle tissue (Amyot et al., 2017; MacMillan et al., 2017; Lortholarie et al., 2021; Marginson et al., 2023; Santos et al., 2023; Labassa et al., 2023). Indeed, studies investigating on the REE organotropism have shown that the highest concentrations were recorded in the liver followed by the gills and kidneys of *A. anguilla* (Lortholarie et al., 2021), as well as of *S. solea* (Labassa et al., 2023).

3.2.2. REE distribution

The individual REE distribution estimated in muscle and gonads (Fig. 7, Table S10) appeared similar to the REE distribution patterns measured in the whole organism of fish (Fig. 3) with a contribution of LREEs higher than HREEs, then MREEs, which is consistent with the literature (Squadrone et al., 2019; Lortholarie et al., 2021; Labassa et al., 2023). The distribution was homogenous among all the fish species for both muscle and gonads, except for *P. flesus*, showing for both tissues a higher contribution of MREEs. This difference was explained by a higher Gd contribution reaching 8.6 % compared to the average of 4.3 ± 1.3 % for the muscle of the other species. About the gonads, the MREE contribution reached 10 % *vs* 3.0 ± 1.0 % in the other species. It was also noticeable for all studied species that Y contribution was higher in gonads compared to muscle (13.4 to 18.7 % and 8.0 to 12.4 %, respectively). Nevertheless, contrarily to the study of Lortholarie et al. (2021), highlighting a high contribution of Gd in gonads of *A. anguilla* female organisms collected from the Loire estuary, no predominance of Gd was highlighted in *A. anguilla* gonads of this study. The nonidentification of organisms' gender, as well as the low number of gonad samples of the present study (2 *vs* 14 in Lortholarie et al. (2021)) could explain these diverging results.

3.2.3. Eu, Gd, Tb and Lu anomalies

REE concentrations in muscle and gonads were normalized to PAAS (Fig. S3). Muscle patterns of all fish seemed similar to the patterns of the whole organisms (Fig. 4), with positive Eu, Gd, Tb and Lu anomalies (Fig. S3A). For gonads, the quantification of all REEs was not systematically possible (Table S5) which explains why the REE patterns were not complete for this tissue. However, they still allowed to highlight Gd anomalies in *P. flesus* and *A. anguilla* (Fig. S3B).

The comparison of the quantification of Eu, Gd, Tb and Lu anomalies did not highlight any differences between the whole organism and the muscle in a fish species, except for *C. ramada* and *P. flesus*. *C. ramada* showed significantly higher Eu anomalies in the muscle (2.31 ± 1.15) than in the whole organism (1.44 ± 0.72) and *P. flesus* displayed significantly lower Tb anomaly values in the muscle (0.71 ± 0.22) compared to the whole organism (1.33 ± 0.54). The muscle anomaly values were not significantly different among the studied fish species, except for Eu showing significantly lower values in *S. solea* compared to *T. luscus* and Tb with significantly lower values in *P. flesus* and *S. solea* than in *T. luscus*. Concerning gonads, *A. anguilla* showed a higher Gd anomaly value in gonads (5.58) compared to the muscle (1.08 ± 0.35) or the whole organism (1.28 ± 0.59), but this could not be statistically tested because of the absence of replicates (Fig. S4, Table S9). As mentioned before, these anomalies could be explained either by the high REE exposure levels of the fish species through the water column due to their lifestyle, or by the possible preferential bioaccumulation or less effective elimination of Eu, Gd, Tb and Lu, induced by species-specific internalization processes. These observations are also consistent with the current uses of the four REEs presenting anomalies (Eu, Gd, Tb and Lu), which are widely used in the industry and medical fields (Bru et al., 2015; Emmett et al., 2017; Müller et al., 2018; Blomqvist et al., 2022) and more pretending to end up in the aquatic ecosystems through wastewater (Verplanck et al., 2010). However, Gd anomaly values recorded in gonads are to be carefully considered since many REEs could not be quantified that may have influenced the polynomial fit of the spectrum pattern.

3.3. Trophic dilution of REE along the food web

The trophic position of the studied species was estimated based on values of stable nitrogen and carbon isotopes ($\delta^{15}N$ and $\delta^{13}C$) which characterize the trophic level of organisms and the distribution of species along the estuary, respectively (Fig. S5, Table S2). These results allowed to evaluate the trophic transfer of REEs along the food web by estimating the TMS based on the linear regression of $\log_{10}[\Sigma REE]$

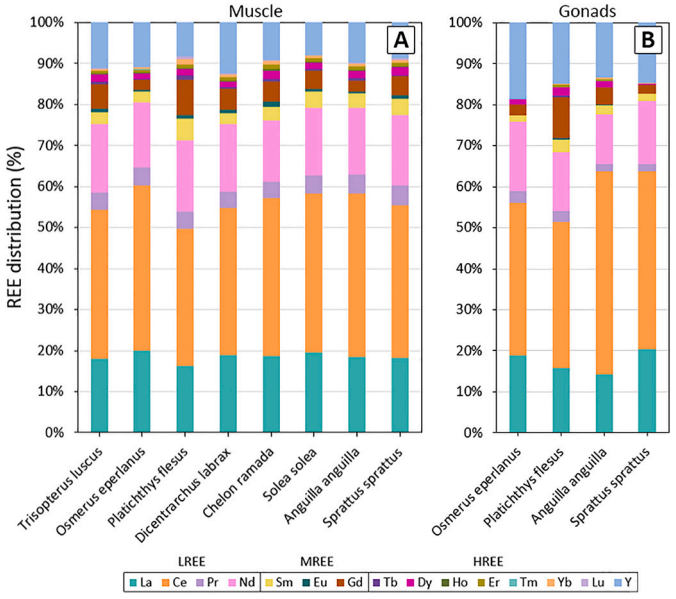

Fig. 7. REE distribution (%) in the muscle (A) and gonads (B) of the vertebrates from the Loire estuary food web.

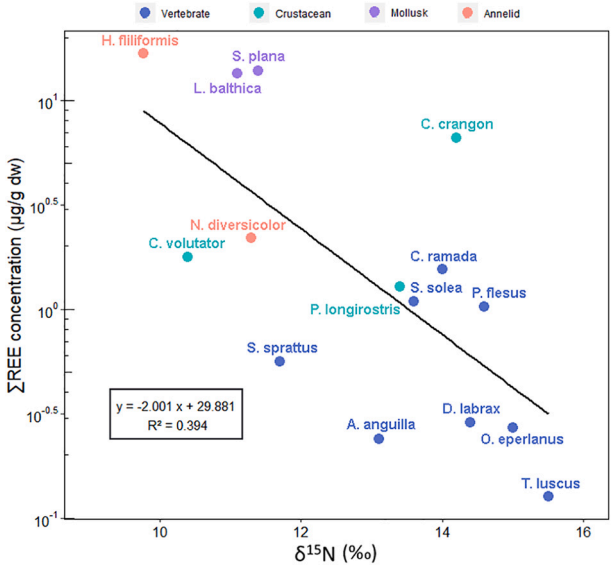

Fig. 8. Linear regression for ΣREE concentrations (log_{10}-scaled axis, µg/g dw) *versus* $\delta^{15}N$ (‰) in organisms from the Loire estuary food web (Pearson correlation test, *p-value* = 0.012). Trophic magnification slope (TMS) which is an indicator of the biomagnification potential was quantified as −2.0.

related to $\delta^{15}N$. The observation of the results and the negative TMS (−2.0) demonstrated higher REE concentrations in organisms from lower trophic levels compared to organisms of higher trophic levels, highlighting a trophic dilution (Fig. 8). This observation was confirmed by the negative significant correlation of individual REE concentrations with $\delta^{15}N$ (Table S11) and is consistent with works already published on the distribution of REEs in other aquatic food webs, either from marine (Wang et al., 2019; Santos et al., 2023) or freshwater (Amyot et al., 2017) ecosystems, as well as in terrestrial ones (MacMillan et al., 2017). The TMS value is, however, higher in the present study than values reported in food webs from temperate lakes of Quebec (−0.59), from the Mulan Bay of China (−0.21) and from the Subae estuary in Brazil (−0.31) (Amyot et al., 2017; Wang et al., 2019; Santos et al., 2023). Moreover, as organisms from lower trophic levels, such as bivalves, tend to preferentially accumulate REEs, they might be selected for environmental biomonitoring.

4. Conclusion

This study demonstrated a phenomenon of trophic dilution of REEs in the food web of the Loire estuary, with the lowest concentrations recorded in the vertebrate phylum and the highest in the primary producers. This is comparable to previous studies on the REE concentrations in trophic chains. REE contribution was the most important for LREEs compared to HREEs and MREEs for all studied species which is consistent with their natural known abundance and their probable bioavailability in the environment. Anomalies were reported in most of the studied species for Eu, Gd, Tb and Lu. For Eu and Gd, this observation is consistent with the anomalies observed in the dissolved phase of the estuary and supposes a higher bioavailability of geogenic Eu(II) and a possible anthropogenic origin for Gd, considering its medical use. The magnitude of the concentrations and the anomalies differing between species (lowest concentrations in vertebrates but highest anomalies) demonstrates the importance of the habitat, the food habits and the species physiology on the bioconcentration. On the other hand, the investigation on fish tissue highlighted higher accumulation of REEs in the whole organism, containing internal organs, and in the gonads compared to the muscle. REE concentrations measured in the several studied organisms were globally higher than those found in other studies, demonstrating a possible contamination of the ecosystem and a high REE exposure of these aquatic organisms. This exposure could lead to a bioaccumulation inducing potential adverse effects, such as oxidative stress, cellular damage or growth inhibition. This study, including a total of twenty-one species representatives of 6 different phyla, provides new data on the bioaccumulation and the trophic transfer of REEs within an estuarine ecosystem and could serve the establishment of environmental thresholds for REEs.

CRediT authorship contribution statement

Julie Rétif: Conceptualization, Data curation, Formal analysis, Investigation, Validation, Visualization, Writing – original draft. **Aurore Zalouk-Vergnoux:** Conceptualization, Project administration, Resources, Supervision, Validation, Writing – review & editing. **Abderrahmane Kamari:** Investigation, Resources. **Nicolas Briant:** Conceptualization, Resources, Supervision, Validation, Writing – review & editing. **Laurence Poirier:** Conceptualization, Funding acquisition, Project administration, Resources, Supervision, Validation, Writing – review & editing.

Declaration of competing interest

The authors declare that they have no known competing financial interests or personal relationships that could have appeared to influence the work reported in this paper.

Data availability

Data will be made available on request.

Acknowledgement

This project was supported by the Observatory of the Sciences of the Universe Nantes Atlantique (OSUNA, Nantes University, CNRS UAR-3281, UGE, CNAM, univ. Angers, IMT Atlantique). The authors thank the French MESRI for the PhD scholarship of J. Rétif. We would also thank the Bio-littoral team as well as A. Baltzer for the sampling of organisms and *Haploops sp.* tubes. Furthermore, we acknowledge Y. François and P. Gaudin for providing technical assistance during the ICP-MS analysis and the freeze-drying process respectively, as well as S. Bruzac and T. Sireau from Ifremer for the treatment of haploops samples, V. Lamabecque for furnishing a ball mill and J. Dumay for the help with algae identification. Finally, we thank the interns M. Olivier, C. Grosgeorge, F. Mohamed Dahlan and S. Graille for the help with sample preparation.

Appendix A. Supplementary data

Supplementary data to this article can be found online at https://doi.org/10.1016/j.scitotenv.2023.169652.

References

Akagi, T., Edanami, K., 2017. Sources of rare earth elements in shells and soft-tissues of bivalves from Tokyo Bay. Mar. Chem. 194, 55–62. https://doi.org/10.1016/j.marchem.2017.02.009.

Alibo, D.S., Nozaki, Y., 1999. Rare earth elements in seawater: particle association, shale-normalization, and Ce oxidation. Geochim. Cosmochim. Acta 63, 363–372. https://doi.org/10.1016/S0016-7037(98)00279-8.

Amyot, M., Clayden, M.G., Macmillan, G.A., Perron, T., Arscott-Gauvin, A., 2017. Fate and trophic transfer of rare earth elements in temperate lake food webs. Environ. Sci. Tech. 51 (11), 6009–6017. https://doi.org/10.1021/acs.est.7b00739.

de Baar, H.J.W., Brewer, P.G., Bacon, M.P., 1985. Anomalies in rare earth distributions in seawater: Gd and Tb*. Geochim. Cosmochim. Acta 49, 1961–1969. https://doi.org/10.1016/0016-7037(85)90090-0.

Barry, M.J., Meehan, B.J., 2000. The acute and chronic toxicity of lanthanum to Daphnia carinata. Chemosphere 41, 1669–1674. https://doi.org/10.1016/S0045-6535(00)00091-6.

Bau, M., Dulski, P., 1996. Anthropogenic origin of positive gadolinium anomalies in river waters. Earth Planet. Sci. Lett. 143, 245–255. https://doi.org/10.1016/0012-821X(96)00127-6.

Benaltabet, T., Gutner-Hoch, E., Torfstein, A., 2021. Heavy metal, rare earth element and Pb isotope dynamics in mussels during a depuration experiment in the Gulf of Aqaba, Northern Red Sea. Front. Mar. Sci. 8 https://doi.org/10.3389/fmars.2021.669329.

Blaise, C., Gagné, F., Harwood, M., Quinn, B., Hanana, H., 2018. Ecotoxicity responses of the freshwater cnidarian Hydra attenuata to 11 rare earth elements. Ecotoxicol. Environ. Saf. 163, 486–491. https://doi.org/10.1016/j.ecoenv.2018.07.033.

Blomqvist, L., Nordberg, G.F., Nurchi, V.M., Aaseth, J.O., 2022. Gadolinium in medical imaging - usefulness, toxic reactions and possible countermeasures - a review. Biomolecules 12 (6). https://doi.org/10.3390/biom12060742.

Bonnail, E., Pérez-López, R., Sarmiento, A.M., Nieto, J.M., DelValls, T.Á., 2017. A novel approach for acid mine drainage pollution biomonitoring using rare earth elements bioaccumulated in the freshwater clam Corbicula fluminea. J. Hazard. Mater. 338, 466–471. https://doi.org/10.1016/j.jhazmat.2017.05.052.

Borrego, J., López-González, N., Carro, B., Lozano-Soria, O., 2004. Origin of the anomalies in light and middle REE in sediments of an estuary affected by phosphogypsum wastes (south-western Spain). Mar. Pollut. Bull. 49, 1045–1053. https://doi.org/10.1016/j.marpolbul.2004.07.009.

Briant, N., Le Monier, P., Bruzac, S., Sireau, T., Araújo, D.F., Grouhel, A., 2021. Rare earth element in bivalves' soft tissues of French metropolitan coasts: spatial and temporal distribution. Arch. Environ. Contam. Toxicol. 81 (4), 600–611. https://doi.org/10.1007/s00244-021-00821-7.

Brito, P., Prego, R., Mil-Homens, M., Caçador, I., Caetano, M., 2018. Sources and distribution of yttrium and rare earth elements in surface sediments from Tagus estuary, Portugal. Sci. Total Environ. 621, 317–325. https://doi.org/10.1016/j.scitotenv.2017.11.245.

Bru, K., Christmann, P., Labbé, J.F., Lefebvre, G., 2015. Panorama 2014 du marché des Terres Rares Rapport public.

Cánovas, C.R., Basallote, M.D., Macías, F., 2020. Distribution and availability of rare earth elements and trace elements in the estuarine waters of the Ría of Huelva (SW Spain). Environ. Pollut. 267 https://doi.org/10.1016/j.envpol.2020.115506.

Cardon, P.Y., Triffault-Bouchet, G., Caron, A., Rosabal, M., Fortin, C., Amyot, M., 2019. Toxicity and subcellular fractionation of yttrium in three freshwater organisms: daphnia magna, chironomus riparius, and oncorhynchus mykiss. ACS Omega 4 (9), 13747–13755. https://doi.org/10.1021/acsomega.9b01238.

Cardon, P.Y., Roques, O., Caron, A., Rosabal, M., Fortin, C., Amyot, M., 2020. Role of prey subcellular distribution on the bioaccumulation of yttrium (Y) in the rainbow trout. Environ. Pollut. 258 https://doi.org/10.1016/j.envpol.2019.113804.

Castor, S.B., Hedrick, J.B., 2006. Rare earth elements. Industrial Minerals and Rocks 7, 769–792.

Censi, P., Mazzola, S., Sprovieri, M., Bonanno, A., Patti, B., Punturo, R., Spoto, S.E., Saiano, F., Alonzo, G., 2004. Rare earth elements distribution in seawater and suspended particulate of the Central Mediterranean Sea. Chem. Ecol. 20 (5), 323–343. https://doi.org/10.1080/02757540410001727954.

Censi, P., Sprovieri, M., Saiano, F., Di Geronimo, S.I., Larocca, D., Placenti, F., 2007. The behaviour of REEs in Thailand's Mae Klong estuary: suggestions from the Y/Ho ratios and lanthanide tetrad effects. Estuar. Coast. Shelf Sci. 71 (3–4), 569–579. https://doi.org/10.1016/j.ecss.2006.09.003.

Censi, P., Randazzo, L.A., D'Angelo, S., Saiano, F., Zuddas, P., Mazzola, S., Cuttitta, A., 2013. Relationship between lanthanide contents in aquatic turtles and environmental exposures. Chemosphere 91 (8), 1130–1135. https://doi.org/10.1016/j.chemosphere.2013.01.017.

Chi, G., Liu, B., Hu, K., Yang, J., He, B., 2021. Geochemical composition of sediments in the Liao River Estuary and implications for provenance and weathering. Reg. Stud. Mar. Sci. 45, 101833 https://doi.org/10.1016/j.rsma.2021.101833.

Christie, T., Brathwaite, B., Tulloch, A., 1998. Mineral commodity report 17 - rare earths and related elements. New Zealand Mining 24 (7), 1–13.

da Costa, A.R.B., Rousseau, T.C.C., Maia, P.D., Amorim, A.M., Sodré, F.F., Teixeira, C.E.P., 2021. Anthropogenic gadolinium in estuaries and tropical Atlantic coastal waters from Fortaleza, Northeast Brazil. Appl. Geochem. 127 https://doi.org/10.1016/j.apgeochem.2021.104908.

Elbaz-Poulichet, Coise, Seidel, J.-L., Othoniel, C., 2002. Occurrence of an anthropogenic gadolinium anomaly in river and coastal waters of Southern France. Water Res. 36, 1102–1105. https://doi.org/10.1016/S0043-1354(01)00370-0.

Emmett, L., Willowson, K., Violet, J., Shin, J., Blanksby, A., Lee, J., 2017. Lutetium 177 PSMA radionuclide therapy for men with prostate cancer: a review of the current literature and discussion of practical aspects of therapy. J. Med. Radiat. Sci. 64 (1), 52–60. https://doi.org/10.1002/jmrs.227.

Figueiredo, C., Oliveira, R., Lopes, C., Brito, P., Caetano, M., Raimundo, J., 2022. Rare earth elements biomonitoring using the mussel Mytilus galloprovincialis in the Portuguese coast: seasonal variations. Mar. Pollut. Bull. 175 https://doi.org/10.1016/j.marpolbul.2022.113335.

Fournier, E., Adam, C., Massabuau, J.C., Garnier-Laplace, J., 2005. Bioaccumulation of waterborne selenium in the Asiatic clam Corbicula fluminea: influence of feeding-induced ventilatory activity and selenium species. Aquat. Toxicol. 72 (3), 251–260. https://doi.org/10.1016/j.aquatox.2005.01.002.

Freitas, R., Costa, S., Cardoso, D., C.E., Morais, T., Moleiro, P., Matias, A.C., Pereira, A.F., Machado, J., Correia, B., Pinheiro, D., Rodrigues, A., Colónia, J., Soares, A.M.V.M., Pereira, E., 2020. Toxicological effects of the rare earth element neodymium in Mytilus galloprovincialis. Chemosphere 244. https://doi.org/10.1016/j.chemosphere.2019.125457.

de Freitas, T.O.P., Pedreira, R.M.A., Hatje, V., 2021. Distribution and fractionation of rare earth elements in sediments and mangrove soil profiles across an estuarine gradient. Chemosphere 264. https://doi.org/10.1016/j.chemosphere.2020.128431.

Fu, F., Akagi, T., Yabuki, S., Iwaki, M., Ogura, N., 2000. Distribution of rare earth elements in seaweed: implication of two different sources of rare earth elements and silicon in seaweed. J. Phycol. 36, 62–70. https://doi.org/10.1046/j.1529-8817.2000.99022.x.

Goldstein, S.J., Jacobsen, S.B., 1988. Rare earth elements in river waters. Earth Planet. Sci. Lett. 89, 35–47.

Gravina, M., Pagano, G., Oral, R., Guida, M., Toscanesi, M., Siciliano, A., Di Nunzio, A., Burić, P., Lyons, D.M., Thomas, P.J., Trifuoggi, M., 2018. Heavy rare earth elements affect sphaerechinus granularis sea urchin early life stages by multiple toxicity endpoints. Bull. Environ. Contam. Toxicol. 100 (5), 641–646. https://doi.org/10.1007/s00128-018-2309-5.

Hanana, H., Turcotte, P., Dubé, M., Gagnon, C., Gagné, F., 2018. Response of the freshwater mussel, Dreissena polymorpha to sub-lethal concentrations of samarium and yttrium after chronic exposure. Ecotoxicol. Environ. Saf. 165, 662–670. https://doi.org/10.1016/j.ecoenv.2018.09.047.

Hatje, V., Bruland, K.W., Flegal, A.R., 2016. Increases in anthropogenic gadolinium anomalies and rare earth element concentrations in San Francisco Bay over a 20 year record. Environ. Sci. Tech. 50 (8), 4159–4168. https://doi.org/10.1021/acs.est.5b04322.

Kawasaki, A., Kimura, R., Arai, S., 1998. Rare earth elements and other trace elements in wastewater treatment sludges. Soil Sci. Plant Nutr. 44 (3), 433–441. https://doi.org/10.1080/00380768.1998.10414465.

Kulaksiz, S., Bau, M., 2013. Anthropogenic dissolved and colloid/nanoparticle-bound samarium, lanthanum and gadolinium in the Rhine River and the impending destruction of the natural rare earth element distribution in rivers. Earth Planet. Sci. Lett. 362, 43–50. https://doi.org/10.1016/j.epsl.2012.11.033.

Kümmerer, K., Helmers, E., 2000. Hospital effluents as a source of gadolinium in the aquatic environment. Environ. Sci. Tech. 34 (4), 573–577. https://doi.org/10.1021/es990633h.

Labassa, M., Pereto, C., Schäfer, J., Hani, Y.M.I., Baudrimont, M., Bossy, C., Dassié, É.P., Mauffret, A., Deflandre, B., Grémare, A., Coynel, A., 2023. First assessment of rare earth element organotropism in Solea solea in a coastal area: the west Gironde mud patch (France). Mar. Pollut. Bull. 197, 115730 https://doi.org/10.1016/j.marpolbul.2023.115730.

Lachaux, N., Otero-Fariña, A., Minguez, L., Sohm, B., Rétif, J., Châtel, A., Poirier, L., Devin, S., Pain-Devin, S., Gross, E.M., Giamberini, L., 2023. Fate, subcellular distribution and biological effects of rare earth elements in a freshwater bivalve under complex exposure. Sci. Total Environ. 905 https://doi.org/10.1016/j.scitotenv.2023.167302.

Le Croizier, G., Lacroix, C., Artigaud, S., Le Floch, S., Munaron, J.-M., Raffray, J., Penicaud, V., Rouget, M.-L., Laë, R., Luis, T. de M., 2019. Metal subcellular partitioning determines excretion pathways and sensitivity to cadmium toxicity in two marine fish species. Chemosphere 217, 754–762. https://doi.org/10.1016/j.chemosphere.2018.10.212.

Lerat-Hardy, A., Coynel, A., Dutruch, L., Pereto, C., Bossy, C., Gil-Diaz, T., Capdeville, M. J., Blanc, G., Schäfer, J., 2019. Rare earth element fluxes over 15 years into a major European estuary (Garonne-Gironde, SW France): hospital effluents as a source of increasing gadolinium anomalies. Sci. Total Environ. 656, 409–420. https://doi.org/10.1016/j.scitotenv.2018.11.343.

Li, J.X., Zheng, L., Sun, C.J., Jiang, F.H., Yin, X.F., Chen, J.H., Han, B., Wang, X.R., 2016. Study on ecological and chemical properties of rare earth elements in tropical marine organisms. Chin. J. Anal. Chem. 44 (10), 1539–1546. https://doi.org/10.1016/S1872-2040(16)60963-5.

Lortholarie, Marjorie, 2021. Les Terres Rares: Exposition et bioaccumulation de deux espèces clés de l'écosystème estuarien ligérien. Université de Nantes.

Lortholarie, M., Zalouk-Vergnoux, A., Couderc, M., Kamari, A., François, Y., Herrenknecht, C., Poirier, L., 2020. Rare earth element bioaccumulation in the yellow and silver European eel (Anguilla anguilla): A case study in the Loire estuary (France). Sci. Total Environ. 719 https://doi.org/10.1016/j.scitotenv.2019.134938.

Lortholarie, M., Poirier, L., Kamari, A., Herrenknecht, C., Zalouk-Vergnoux, A., 2021. Rare earth element organotropism in European eel (Anguilla anguilla). Sci. Total Environ. 766 https://doi.org/10.1016/j.scitotenv.2020.142513.

MacMillan, G.A., Chételat, J., Heath, J.P., Mickpegak, R., Amyot, M., 2017. Rare earth elements in freshwater, marine, and terrestrial ecosystems in the eastern Canadian Arctic. Environ. Sci.: Processes Impacts 19 (10), 1336–1345. https://doi.org/10.1039/c7em00082k.

Marchand, J., 1981. Observations sur l'écologie de Crangon crangon (Linné) et Palaemon longirostris H. Milne Edwards (Crustacea, Decapoda, Natantia) Estuaire interne de la Loire (France). Vie et Milieu 31 (1), 83–92.

Marginson, H., MacMillan, G.A., Grant, E., Gérin-Lajoie, J., Amyot, M., 2023. Rare earth element bioaccumulation and cerium anomalies in biota from the Eastern Canadian subarctic (Nunavik). Sci. Total Environ. 879 https://doi.org/10.1016/j.scitotenv.2023.163024.

Marmolejo-Rodríguez, A.J., Prego, R., Meyer-Willerer, A., Shumilin, E., Sapozhnikov, D., 2007. Rare earth elements in iron oxy-hydroxide rich sediments from the Marabasco River-estuary system (pacific coast of Mexico). REE affinity with iron and aluminium. J. Geochem. Explor. 94 (1–3), 43–51. https://doi.org/10.1016/j.gexplo.2007.05.003.

Mashitah, S.M., Shazili, N.A.M., Rashid, M.K.A., 2012. Elemental concentrations in Brown seaweed, Padina sp. along the east coast of peninsular Malaysia. Aquat. Ecosyst. Health Manag. 15 (3), 267–278. https://doi.org/10.1080/14634988.2012.705774.

Mayfield, D.B., Fairbrother, A., 2015. Examination of rare earth element concentration patterns in freshwater fish tissues. Chemosphere 120, 68–74. https://doi.org/10.1016/j.chemosphere.2014.06.010.

Mehmood, M., 2018. Rare earth elements- a review. J. Ecol. Nat. Resour. 2 (2) https://doi.org/10.23880/jenr-16000128.
Merschel, G., Bau, M., 2015. Rare earth elements in the aragonitic shell of freshwater mussel Corbicula fluminea and the bioavailability of anthropogenic lanthanum, samarium and gadolinium in river water. Sci. Total Environ. 533, 91–101. https://doi.org/10.1016/j.scitotenv.2015.06.042.
Möller, P., Paces, T., Dulski, P., Morteani, G., 2002. Anthropogenic Gd in surface water, drainage system, and the water supply of the City of Prague, Czech Republic. Environ. Sci. Technol. 36 (11), 2387–2394. https://doi.org/10.1021/es010235q.
Möller, P., Morteani, G., Dulski, P., 2003. Anomalous gadolinium, cerium, and yttrium contents in the Adige and Isarco River waters and in the water of their tributaries (Provinces Trento and Bolzano/Bozen, NE Italy). Acta Hydrochim. Hydrobiol. 31 (3), 225–239. https://doi.org/10.1002/aheh.200300492.
Müller, C., Domnanich, K.A., Umbricht, C.A., Van der Meulen, N.P., 2018. Scandium and terbium radionuclides for radiotheranostics: current state of development towards clinical application. Br. J. Radiol. 91 https://doi.org/10.1259/bjr.20180074.
Naskar, N., Lahiri, S., 2021. Theranostic terbium radioisotopes: challenges in production for clinical application. Front. Med. 8 https://doi.org/10.3389/fmed.2021.675014.
Pereto, C., Coynel, A., Lerat-Hardy, A., Gourves, P.Y., Schäfer, J., Baudrimont, M., 2020. Corbicula fluminea: a sentinel species for urban rare earth element origin. Sci. Total Environ. 732 https://doi.org/10.1016/j.scitotenv.2020.138552.
Perrat, E., Parant, M., Py, J.S., Rosin, C., Cossu-Leguille, C., 2017. Bioaccumulation of gadolinium in freshwater bivalves. Environ. Sci. Pollut. Res. 24 (13), 12405–12415. https://doi.org/10.1007/s11356-017-8869-9.
Pignotti, E., Dinelli, E., Birke, M., 2017. Geochemical characterization and rare earth elements anomalies in surface- and groundwaters of the Romagna area (Italy). Rend. Fis. Acc. Lincei 28, 265–279. https://doi.org/10.1007/s12210-016-0561-3.
Pillai, M.R.A., Knapp, F.F.R., 2015. Evolving important role of Lutetium-177 for therapeutic nuclear medicine. Curr. Radiopharm. 8, 78–85.
Pourmand, A., Dauphas, N., Ireland, T.J., 2012. A novel extraction chromatography and MC-ICP-MS technique for rapid analysis of REE, Sc and Y: revising CI-chondrite and Post-Archean Australian Shale (PAAS) abundances. Chem. Geol. 291, 38–54. https://doi.org/10.1016/j.chemgeo.2011.08.011.
Qiang, T., Xiao-rong, W., Li-qing, T., Le-mei, D., 1994. Bioaccumulation of the rare earth elements lanthanum, gadolinium and yttrium in carp (Cyprinus carpio). Environ. Pollut. 85 (3), 345–350. https://doi.org/10.1016/0269-7491(94)90057-4.
Rabiet, M., Brissaud, F., Seidel, J.L., Pistre, S., Elbaz-Poulichet, F., 2009. Positive gadolinium anomalies in wastewater treatment plant effluents and aquatic environment in the Hérault watershed (South France). Chemosphere 75 (8), 1057–1064. https://doi.org/10.1016/j.chemosphere.2009.01.036.
Reindl, A.R., Falkowska, L., 2021. Trace elements in the muscle, ova and seminal fluid of key clupeid representatives from the Gdansk Bay (South Baltic Sea) and Iberian Peninsula (North-East Atlantic). J. Trace Elem. Med. Biol. 68 https://doi.org/10.1016/j.jtemb.2021.126803.
Rétif, J., Zalouk-Vergnoux, A., Briant, N., Poirier, L., 2023. From geochemistry to ecotoxicology of rare earth elements in aquatic environments: diversity and uses of normalization reference materials and anomaly calculation methods. Sci. Total Environ. 856 https://doi.org/10.1016/j.scitotenv.2022.158890.
Sakamoto, N., Kano, N., Imaizumi, H., 2008. Biosorption of uranium and rare earth elements using biomass of algae. Bioinorg. Chem. Appl. 2008 https://doi.org/10.1155/2008/706240.
Santos, A.C.S.S., Souza, L.A., Araujo, T.G., de Rezende, C.E., Hatje, V., 2023. Fate and trophic transfer of rare earth elements in a tropical estuarine food web. Environ. Sci. Tech. 57 (6), 2404–2414. https://doi.org/10.1021/acs.est.2c07726.
Squadrone, S., Brizio, P., Battuello, M., Nurra, N., Sartor, R.M., Benedetto, A., Pessani, D., Abete, M.C., 2017. A first report of rare earth elements in northwestern Mediterranean seaweeds. Mar. Pollut. Bull. 122 (1–2), 236–242. https://doi.org/10.1016/j.marpolbul.2017.06.048.
Squadrone, S., Nurra, N., Battuello, M., Mussat Sartor, R., Stella, C., Brizio, P., Mantia, M., Pessani, D., Abete, M.C., 2018. Trace elements, rare earth elements and inorganic arsenic in seaweeds from Giglio Island (Thyrrenian Sea) after the Costa Concordia shipwreck and removal. Mar. Pollut. Bull. 133, 88–95. https://doi.org/10.1016/j.marpolbul.2018.05.028.
Squadrone, S., Brizio, P., Stella, C., Mantia, M., Battuello, M., Nurra, N., Sartor, R.M., Orusa, R., Robetto, S., Brusa, F., Mogliotti, P., Garrone, A., Abete, M.C., 2019. Rare earth elements in marine and terrestrial matrices of northwestern Italy: implications for food safety and human health. Sci. Total Environ. 660, 1383–1391. https://doi.org/10.1016/j.scitotenv.2019.01.112.
Tepe, N., Bau, M., 2016. Behavior of rare earth elements and yttrium during simulation of arctic estuarine mixing between glacial-fed river waters and seawater and the impact of inorganic (nano-)particles. Chem. Geol. 438, 134–145. https://doi.org/10.1016/j.chemgeo.2016.06.001.
Thibault de Chanvalon, A., Metzger, E., Mouret, A., Knoery, J., Chiffoleau, J.F., Brach-Papa, C., 2016. Particles transformation in estuaries: Fe, Mn and REE signatures through the Loire estuary. J. Sea Res. 118, 103–112. https://doi.org/10.1016/j.seares.2016.11.004.
Thomsen, H.S., 2017. Are the increasing amounts of gadolinium in surface and tap water dangerous? Acta Radiol. 58 (3), 259–263. https://doi.org/10.1177/0284185116666419.
Verplanck, P.L., Furlong, E.T., Gray, J.L., Phillips, P.J., Wolf, R.E., Esposito, K., 2010. Evaluating the behavior of gadolinium and other rare earth elements through large metropolitan sewage treatment plants. Environ. Sci. Tech. 44 (10), 3876–3882. https://doi.org/10.1021/es903888t.
Wang, Z., Yin, L., Xiang, H., Qin, X., Wang, S., 2019. Accumulation patterns and species-specific characteristics of yttrium and rare earth elements (YREEs) in biological matrices from Maluan Bay, China: implications for biomonitoring. Environ. Res. 179 https://doi.org/10.1016/j.envres.2019.108804.
Wang, Z., Shu, J., Wang, Z., Qin, X., Wang, S., 2022. Geochemical behavior and fractionation characteristics of rare earth elements (REEs) in riverine water profiles and sentinel clam (Corbicula fluminea) across watershed scales: insights for REEs monitoring. Sci. Total Environ. 803 https://doi.org/10.1016/j.scitotenv.2021.150090.
Yang, L., Wang, X., Nie, H., Shao, L., Wang, G., Liu, Y., 2016. Residual levels of rare earth elements in freshwater and marine fish and their health risk assessment from Shandong, China. Mar. Pollut. Bull. 107 (1), 393–397. https://doi.org/10.1016/j.marpolbul.2016.03.034.
Zhang, Y., Gao, X., Arthur Chen, C.T., 2014. Rare earth elements in intertidal sediments of Bohai Bay, China: concentration, fractionation and the influence of sediment texture. Ecotoxicol. Environ. Saf. 105 (1), 72–79. https://doi.org/10.1016/j.ecoenv.2014.04.006.
Zhao, L., Liu, L., 2018. Assessing the impact of lanthanum on the bivalve Corbicula fluminea in the Rhine River. Sci. Total Environ. 640–641, 830–839. https://doi.org/10.1016/j.scitotenv.2018.05.351.